

Chapter 5

Aggregation Properties of Mixed Surfactant System of Dimeric Butane-1,4- bis(dodecyl hydroxyethyl methyl ammonium bromide) and Its Monomeric Counterpart

Contents

	Page no.
5.1 Introduction	166
5.2 Experimental	167
5.2.1 Materials	167
5.2.2 Conductivity	168
5.2.3 Kraft temperature	168
5.2.4 Foamability and foam stability	168
5.2.5 Oil solubilisation capacity	169
5.2.6 Small angle neutron scattering	169
5.3 Results and Discussion	169
5.3.1 Kraft temperature	169
5.3.2 Critical micelle concentration	172
5.3.3 Foamability and oil solubilisation	175
5.3.4 Shape, size and aggregation number	177
Average equilibrium distance	
5.4 Conclusions	183
5.5 Literature Cited	184-185

5.1 Introduction

Since combination of surfactants show synergistic effect in their performance as compared to single surfactant, use of mixed surfactants in industrial applications is extensively reported [1-5]. Recently gemini surfactants have attracted attention due to their unique solution properties [6-13]. In comparison with monomeric surfactants gemini surfactants especially with shorter spacer ($s \leq 5$) possess unusual properties, such as very low CMC, high viscoelasticity and higher aggregation tendency [11-17]. In mixed micellar system containing gemini and monomeric surfactants (16-s-16 DMA and CTAB) decrease in critical micellar concentration and increase in Kraft temperature with increased mol fraction of gemini surfactant was reported by Zhao et al [18]. Schosseler et al [19] through SANS observed that in binary mixtures of 12-2-12 DMA and DTAB micelles progressively change from the ellipsoidal to spheroidal shapes with increase in the mole fraction of DTAB. Variation in size, shape and aggregation tendency was reported to be strongly dependent upon molecular architecture and composition of mixed surfactant systems and experimental conditions such as concentration and temperature [20-22].

Recently we have reported the effect of head group polarity and spacer length on aggregation behavior of novel bisquaternary ammonium surfactant with $C_{12/16}$ alkyl chain through conductance, viscosity, surface tension and SANS studies [23-26]. CMC values were observed to decrease 100 times and micelles showed higher aggregation tendency when head group polarity of conventional dimeric surfactant 12/16-s-12/16 DMA (where DMA is dimethyl amine and $s = 4, 6, 8$ & 10), increased on successive replacement of $-CH_3$ group by $-C_2H_4OH$ groups.

Hence in this section we have undertaken a study of mixed micellar systems containing bis-quaternary ammonium surfactant 12-4-12 MEA and its monomeric counterpart (C_{12} DMEAB) through SANS and conductivity measurements.

The structures of dimeric and monomeric surfactants used in present study are given below

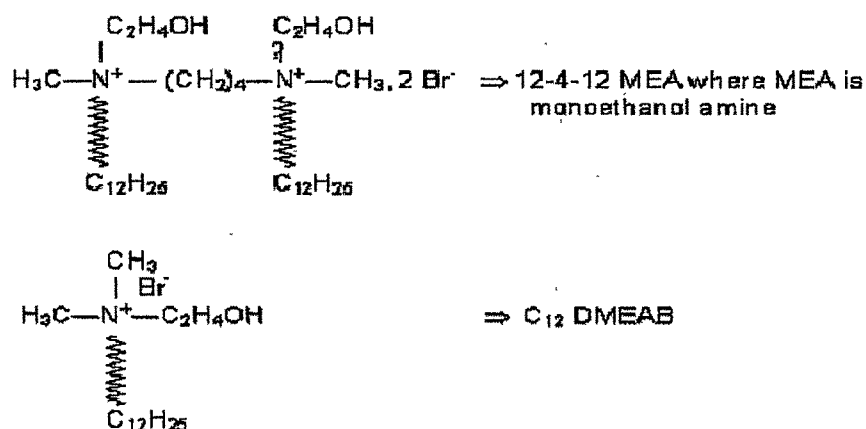


Chart: Chemical structures of surfactants under study

5.2 Experimental

5.2.1 Materials

The novel bis-quaternary ammonium surfactant 12-4-12 MEA and its monomeric counterpart C₁₂DMEAB were synthesized as described earlier in section 2.2.1. AR grade solvents and reagents were used through out the work. Solutions for SANS studies were prepared in D₂O (at least 99 atom % D) obtained from Heavy Water Division, Bhabha Atomic Research Centre, Mumbai, India. Double-distilled and deionized water was used for all physicochemical studies.

5.2.2 Kraft Temperature

The Kraft temperature (k_T) for the mixed surfactant system of 12-4-12 MEA and C_{12} DMEAB was determined through conductance measurements as well as visual observation of the transparency of the system. Aqueous one percent (w/v) true solutions of pure and mixed surfactants were prepared and placed in refrigerator at a temperature $1 - 2^\circ\text{C}$ for at least 24 h, till precipitate of the hydrated surfactant crystals appeared. The precipitated system was introduced in conductivity cell and temperature of the system was gradually increased using water bath of accuracy $\pm 0.2^\circ\text{C}$. The conductance was measured as the temperature was progressively increased until the turbid solutions became transparent. The Kraft temperature was taken as the temperature where the conductance (k) versus T plot (Figure 5.1) showed break and solutions were transparent. This break usually coincided with the temperature where complete dissolution of hydrated solid surfactant resulted into transparent solution. The measurements were repeated at least three times and reproducibility in k_T values was observed within $\pm 0.3^\circ\text{C}$.

5.2.3 Conductivity

Critical micelle concentration of the mixed surfactant system was determined through conductance measurements as a function of total surfactant concentration, using Digital Conductivity Meter-664 (Equiptronic, Mumbai, India) with cell constant 1.01 cm^{-1} , at $30.0 \pm 0.1^\circ\text{C}$. The average degree of dissociation of counter ions (α_{ave}) of the micelle and CMC were determined from specific conductance (k) vs concentration (C) plots (Figure 5.2).

5.2.4 Foamability and Foam Stability

Foamability and foam stability of mixed surfactant systems were studied as per the method reported by Shah and coworker [27, 28]. A graduated glass cylinder of 100 cm^3 volume was used for the measurement of the foam stability and

foamability. Twenty cubic centimeters 1 % (w/v) surfactant solution was poured into the calibrated cylinder. The solution was given 10 uniform jerks within 10 s. The volume of the foam generated was measured as foamability and the time required for the collapse of the foam to half of its initial height was taken as a measure for the foam stability. The experiments were repeated at least five times.

5.2.5 Oil Solubilisation Capacity

A mixed micellar systems containing various mole fractions of 12-4-12 MEA and its monomeric counterpart C₁₂DMEAB, at constant total surfactant concentration of 0.2 M were prepared. Solutions were thoroughly homogenized using a vortex mixer and kept in a thermostated water bath at 30 ± 0.1 °C. These mixtures were then titrated with methyl methacrylate (oil) using a micro-burette.

5.2.6 Small Angle Neutron Scattering

Small angle neutron scattering studies were performed as described in section 2.2.9. The scattering intensities from the mixed surfactant solutions were corrected for detector background sensitivity, empty cell scattering and sample transmission. Scattering intensity of solvent was subtracted from that of the sample. The resulting corrected intensities were normalized to absolute cross section units, and thus $d\Sigma/d\Omega$ vs Q were obtained. This absolute calibration has an estimated uncertainty of 10 %. The experimental values were fitted using nonlinear least-square method.

5.3. Results and Discussion

5.3.1 Kraft Temperature

The determination of Kraft temperature through conductance measurements is superior to the commonly used method of visual observation which is dependent

on the judgment of the observer. Hence Kraft temperatures (k_T) of binary mixtures of 12-4-12 MEA and C₁₂DMEAB surfactant systems were measured as a function of increased mole fraction of 12-4-12 MEA by using conductance measurement. From the Figure 5.1 it was observed that conductance increases rapidly with increase in temperature due to dissolution of the hydrated crystal of surfactant, until Kraft temperature reaches. Thereafter the conductance increases slowly only due to the increase in the mobility of ions with increase in temperature. The Kraft temperature determined for the mixed surfactant systems is given in Table 5.1. Kraft temperature was observed to increase with mole fraction of 12-4-12 MEA.

This fact can be explained in terms of contributions of hydrophobic and electrostatic interactions on micellization and hence on kraft temperature. It has been reported that increase in hydrophobicity of alkyl chain length in a surfactant molecule assists in micellization. It is also reported that increase in alkyl chain length increases kraft temperature [30]. This means increase in micellization tendency is related to kraft temperature. If we consider electrostatic interactions which usually decrease with the addition of gemini surfactant (as α decreases, Table 5.3) would also assist in micellization. Therefore decrease in charge of head group facilitates micellization. Taking the analogy from the above two facts one can understand that decrease in charge should increase the kraft temperature of the system as this would increase micellization tendency as observed in the present system (Table 5. 1).

Table 5.1 Effect of mole fraction of 12-4-12 MEA surfactant on Kraft temperature (k_T) of mixed surfactant system 12-4-12 MEA and C_{12} DMEAB.

Mole fraction of 12-4-12 MEA	Kraft Temperature k_T ($^{\circ}\text{C}$)
0.00	8
0.25	16
0.50	18
0.75	20
1.00	30

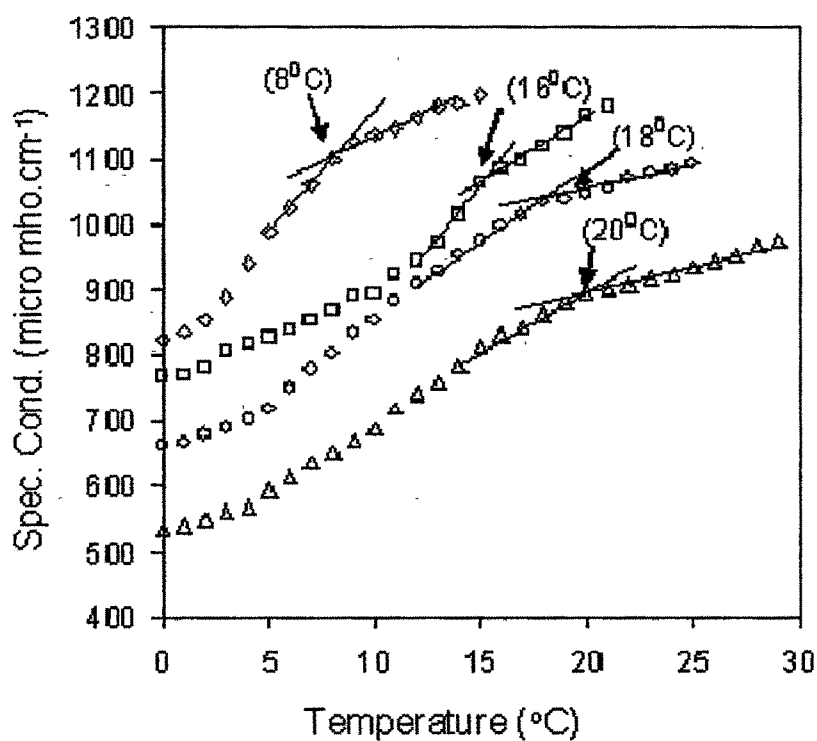


Figure 5.1 Plots of specific conductance against temperature for determination of Kraft temperature (k_T) of mixed surfactant system 12-4-12 MEA and C_{12} DMEAB as a function of mole fraction of 12-4-12 MEA. 0.00 (\diamond), 0.25 (\square), 0.50 (\circ), 0.75 (Δ)

5.3.2 Critical Micelle Concentration

The plots for the conductometric determination of critical micelle concentrations of binary mixtures of 12-4-12 MEA and C₁₂DMEAB, as a function of mole fractions of 12-4-12 MEA (0, 0.25, 0.50, 0.75 and 1.0) are given in Figure 5.2(a). The average degree of dissociation of counter ions (α_{ave}) of the micelle was taken as the ratio of the dk/dc values above and below the CMC. The CMC, average degree of ionization of micelle (α_{ave}) and Gibb's free energy change of micellization (ΔG_m^0) for the mixed surfactant systems were determined from conductance data and results are given in Table 5.2. It was observed that CMC and α_{ave} decrease with increasing mole fraction of 12-4-12 MEA in mixed surfactant system, whereas more negative value of Gibb's free energy change (ΔG_m^0) of micellization, indicates the enhancement in micellization process with increase in mol fraction of 12-4-12 MEA. Introduction of very small fraction of 12-4-12 MEA (0.25) showed drastic decrease in the CMC of mixed surfactant. These results indicate that the 12-4-12 MEA surfactant has more tendency towards micellization than C₁₂DMEAB surfactant.

Clint equation [31] was used to determine the ideal/nonideal behavior of the mixed surfactant system by correlating the theoretical values of CMC* with experimental CMC values through the following equation.

$$1/CMC^* = x_1/c_{m1} + (1 - x_1)/c_{m2} \quad (1)$$

where x_1 is the mole fraction of the 12-4-12 MEA surfactant in the total solute concentration of mixed surfactant system and c_{m1} and c_{m2} are the respective CMC's of the pure individual surfactants 12-4-12 MEA and C₁₂DMEAB. The CMC* values for binary mixtures of 12-4-12 MEA and C₁₂DMEAB calculated using equation 1, were plotted along with experimental CMC values as illustrated in Figure 5.2(b). Good agreement between theoretically calculated and experimentally obtained CMC values was observed particularly at higher mole

fraction of dimeric surfactant in the present mixed surfactant systems, indicating ideal mixing of the surfactants

Table 5.2 Effect of mole fraction of 12-4-12 MEA on the micellar parameters of mixed surfactant systems 30 °C.

Mole fraction of 12-4-12 MEA	CMC (M)	CMC* (M)	α_{ave}	ΔG_m^0 KJ.mol ⁻¹
0.00	$13.6 \pm 0.1 \times 10^{-3}$	$13.6 \pm 0.1 \times 10^{-3}$	0.33	-18.1
0.25	$10.7 \pm 0.1 \times 10^{-5}$	$11.1 \pm 0.1 \times 10^{-5}$	0.29	-27.9
0.50	$5.6 \pm 0.1 \times 10^{-5}$	$5.6 \pm 0.1 \times 10^{-5}$	0.28	-30.0
0.75	$3.6 \pm 0.1 \times 10^{-5}$	$3.7 \pm 0.1 \times 10^{-5}$	0.27	-31.4
1.00	$2.8 \pm 0.1 \times 10^{-5}$	$2.8 \pm 0.1 \times 10^{-5}$	0.26	-32.8

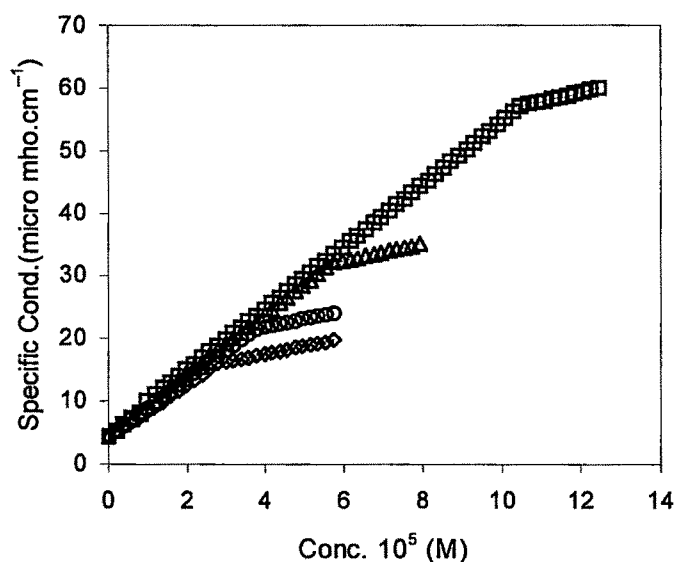


Figure 5.2(a) Plots of specific conductance (k) as a function of total surfactant concentration, $[S]_{\text{tot}}$ at 30 °C at various mole fractions of 12-4-12 MEA, 0.25 (□), 0.50 (Δ), 0.75 (O), 1.00 (◇).

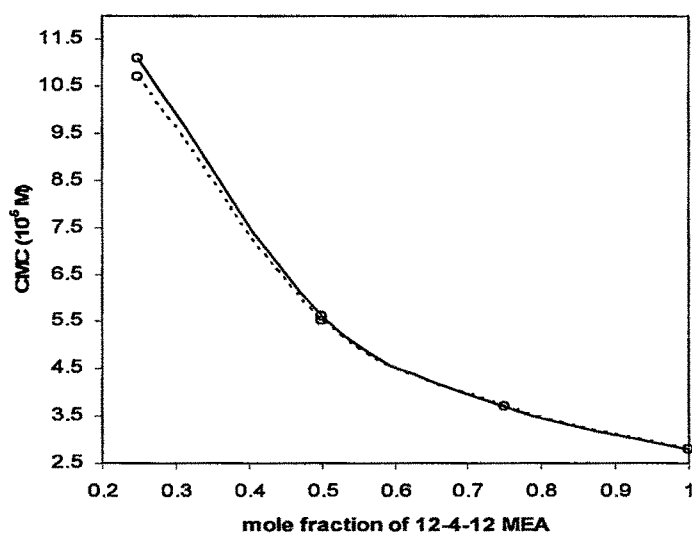


Figure 5.2(b) Plots of CMC against mole fraction of 12-4-12 MEA surfactant in binary mixture of 12-4-12MEA + C₁₂DMEAB at 30 °C. Experimental CMC (dotted line); theoretically calculated CMC* (solid line)

5.3.3 Foamability and Oil Solubilisation

Foamability and foam stability as a function of mole fraction of 12-4-12 MEA in a mixed surfactant system was determined manually by the method reported by Shah [27]. The results are given in Figure 5.3. Foamability was observed to decrease and foam stability was observed to increase with mole fraction of 12-4-12 MEA in the mixed system.

Amount of methyl methacrylate solubilized in a binary micellar system 12-4-12 MEA and C₁₂DMEAB against mole fraction of 12-4-12 MEA is given in Figure 5.4. The oil solubilisation capacity was observed to increase with increased fraction of 12-4-12 MEA in mixed micellar system. This can be attributed to the increased hydrophobicity and increased size of micelle.

Shah and coworker [27,28] reported that the foamability, foam stability and oil solubilization capacity of surfactant are the important properties which are related to micellar stability. Figure 5.3 and 5.4 show, decrease in foamability and increase in oil solubilization capacity with increase of mole fraction of 12-4-12 MEA in mixed surfactant system. This can be attributed to the increased hydrophobicity of mixed surfactant system.

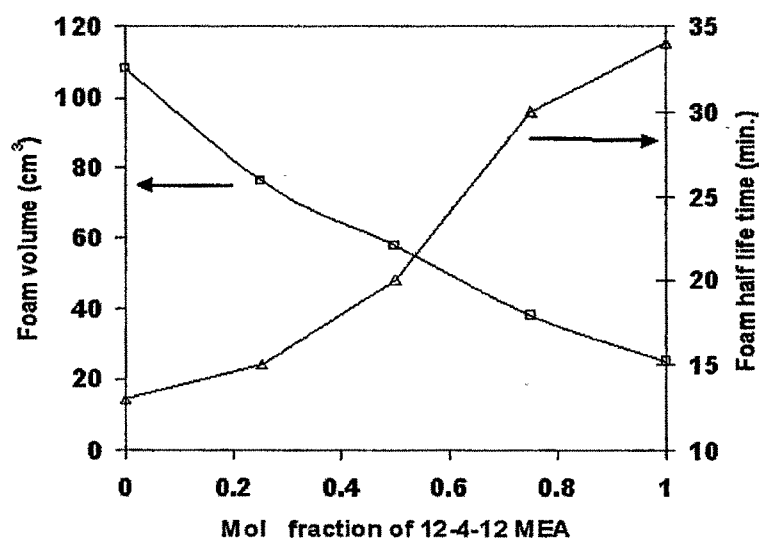


Figure 5.3 Foamability and foam stability as a function of mole fraction of 12-4-12 MEA for mixed surfactant system 12-4-12 MEA and C_{12} DMEAB at 0.2M and 30 °C.
 □ Foamability, Δ Foam stability

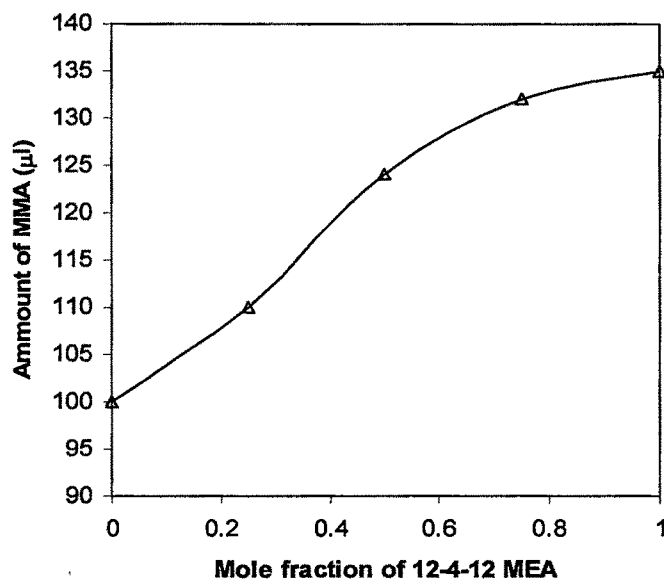


Figure 5.4 Effect of mole fraction of 12-4-12 MEA in binary mixture of C_{12} DMEAB and 12-4-12MEA on the solubilization of methyl methacrylate at 0.2 M concentration and 30°C.

5.3.4 Shape, Size and Aggregation Number

SANS is a well established powerful technique which provides information about shape, size and microenvironment of surfactant aggregates [29, 30]. SANS study of mixed micellar system containing various mole fractions of 12-4-12 MEA and its monomeric counterpart C₁₂DMEAB at constant total surfactant concentration of 0.2 M at 30°C, was done using SANS diffractometer. In SANS, a beam of neutron is directed upon the sample under examination and the scattering intensities of neutron in different directions were measured.

Data Analysis

The coherent differential scattering cross section ($d\Sigma/d\Omega$) for a unit volume of solution of monodispersed mixed micelles is given by [32].

$$d\Sigma/d\Omega = n V_m^2 (\rho_m - \rho_s)^2 P(Q) S(Q) \quad (2)$$

where n denotes the number density of micelles, ρ_m and ρ_s are the scattering length densities of micellar solution and solvent respectively and V_m is the volume of the mixed micelle. The aggregation number (N) of mixed micelles is related to the micelle volume by the relation $N = V_m/v$, where v is volume of the individual surfactant molecule. The volume of mixed micelles is calculated by using equation 3.

$$V_m = N (x_1 v_{\text{dimeric}} + (1 - x_1) v_{\text{monomer}}) \text{ \AA}^3 \quad (3)$$

where v_{dimeric} and v_{monomer} are the volumes of dimeric and its corresponding monomeric surfactant respectively, which were calculated by using Tand-fold formula. $N = (N_{\text{monomer}} + N_{\text{dimeric}})$, where N_{monomer} and N_{dimeric} are the aggregation numbers of monomeric and dimeric surfactants respectively in mixed micelles. x_1 is mole fraction of dimeric surfactant in bulk. The volumes used for 12-4-12 MEA

and C₁₂DMEAB are 1269 and 525 respectively. The scattering length density of mixed micelle solution is obtained from equation 4.

$$\rho_m = (x_1 \rho_{\text{dimeric}} + (1 - x_1) \rho_{\text{monomer}}) \quad (4)$$

where ρ_{dimeric} and ρ_{monomer} are the scattering length densities due to dimeric and monomeric surfactants respectively.

The $P(Q)$ and $S(Q)$ are respectively intra and inter particle structure factors. The intra particle structure factor $P(Q)$ depends on the shape and size of the micelle. Expressions for $P(Q)$ corresponding to different geometrical shapes are reported [33]. In particular, $P(Q)$ for an ellipsoidal micelles is given as.

$$P(Q) = \int [F(Q, \mu)]^2 d\mu \quad (5)$$

where $F(Q, \mu)$ is a form factor and μ is the cosine of the angle between the major axis and wave vector Q . Form factor $F(Q, \mu)$ is calculated as

$$F(Q, \mu) = 3(\sin w - w \cos w)/w^3 \quad (6)$$

where $w = Q [a^2 \mu^2 + b^2 (1 - \mu^2)]^{1/2}$; a and b are respectively the semi minor and semi major axis of the ellipsoidal micelle.

The inter particle structure factor $S(Q)$ for ellipsoidal micelles is calculated using mean spherical approximation as developed by Hayter and Penfold [33]. In SANS data analysis aggregation number (N), fractional charge per head (α) and semi minor axis (a) are taken as fitting parameters. The correlation between calculated and experimental values of scattering intensities is judged by calculating χ^2 values, defined as

$$\chi^2 = (1/M - k) \sum [I_{\text{cal}} - I_{\text{exp}} / \{E(I_{\text{exp}})\}]^2 \quad (7)$$

where M is number of points, k is number of fitting parameters, I is intensities, and E is error in intensity measurements.

The SANS spectra of 12-4-12 MEA and C_{12} DMEAB mixed micellar systems (Fig. 5.5) show well defined correlation peaks characteristics of dispersion of charged particles. These peaks arise because of the corresponding interparticle structure factor $S(Q)$ at $Q_{\max} \simeq 2\pi/D$, where D is the average distance between the micelles. As mol fraction of 12-4-12 MEA in the mixed micellar system increases, the peak position of maximum intensity (Q_{\max}) shifts to lower Q , concurrently with the increase in the maximum intensity (Fig.5.5), indicating the change in number density and geometry of micelles. Experimental values of SANS intensities were best matched with the values obtained by using prolate ellipsoidal model.

The micellar parameters extracted from SANS measurement are given in Table 5.3. A sharp increase in equivalent aggregation number ($N_E = N_{\text{monomer}} + 2N_{\text{dimeric}}$, where the dimeric surfactant is considered to be composed of two monomeric parts) and axial ratio (b/a) of the micelles with increasing mole fraction of 12-4-12 MEA in mixed systems indicate formation of more elongated micelles. Whereas significant decrease in the fractional charge (α) with increasing mol fraction of 12-4-12 MEA in mixed micelle indicates decreased Coulombic repulsion between the charged heads and more tightly packed head groups. Increase in semi minor axis, a (Table 5.3) with increase in mol fraction of 12-4-12 MEA, indicates more tightly packed hydrophobic chains inside the micelle core. This can be attributed, to the increase in hydrophobic attractive interaction between hydrophobic chains.

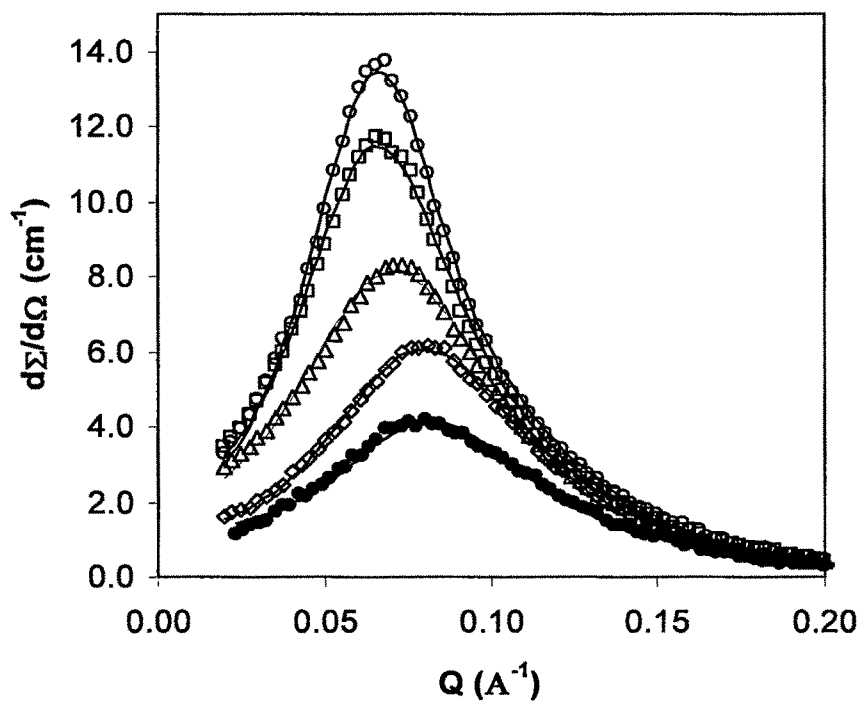


Figure 5.5 SANS spectra from mixed surfactant system [12-4-12 MEA and C₁₂DMEAB] as a function of mole fraction of 12-4-12 MEA at 0.2M concentration and 30°C. Solid lines represent theoretical fits and symbols experimentally determined values.
0.00 (●), 0.25 (◇), 0.50 (Δ), 0.75 (□), 1.00 (○)

Table 5.3 Aggregation parameters for binary mixture of 12-4-12 MEA and C₁₂DMEAB at 0.2M and 30 °C.

Mole frac ¹ 12-4-12 MEA	N _E	N _{C12DMEAB}	N ₁₂₋₄₋₁₂	α	b (Å)	a (Å)	b/a
0.00	67±7	67±7	0	0.15±0.01	34.7±1.5	15.2±0.5	2.28±0.08
0.25	80±9	48±7	16±1	0.14±0.01	38.7±1.8	16.1±0.5	2.40±0.08
0.50	120±12	40±6	40±3	0.09±0.01	51.4±2.2	17.1±0.5	3.01±0.07
0.75	182±16	26±4	78±6	0.09±0.01	72.6±2.8	17.9±0.5	4.06±0.07
1.00	222±20	0	111±10	0.05±0.01	84.5±3.2	18.2±0.5	4.64±0.07

(N_E is the equivalent aggregation number of monomers; i.e., [N_{monomer} + 2N_{dimeric}], N_{monomer} and N_{dimeric} = aggregation nos. of monomeric and dimeric surfactant, α is the fractional charge, 'a' and 'b' are the semi-minor and major axis of micelle respectively)

Average equilibrium distance

In aqueous solution two positively charged heads $[-N^+(C_2H_4OH)(CH_3)]$ of surfactant units tend to maintain a critical distance to overcome the Coulombic repulsion. We have estimated this equilibrium distance (d) from the SANS data, assuming it to be equal to $(4\pi a_{\text{eff}}^2/N)^{1/2}$, where a_{eff} is $(a^2b)^{1/3}$ and considering the micelles to be ellipsoidal. The observed ' d ' value for DTAB was ~ 8.32 Å, which is reasonably in good agreement with the value reported by Zana [11]. In the same way, we calculated the equilibrium distance (d) between the charged heads in mixed micellar systems which are given in Table 5.4. The equilibrium distance ' d ' in mixed micellar system decreases with increasing mol fraction of dimeric surfactant affecting the packing curvature of micelle resulting in the change in geometry of mixed micelles.

Table 5.4 Effective head group area (A) and equilibrium distance (d) between charged heads within micelle of mixed surfactant system [12-4-12 MEA + C_{12} DMEAB] at 0.2 M concentration and 30°C.

Mol fraction of 12-4-12 MEA	Average distance between charged head groups d (Å)	Effective head group area A (Å ²)
0.00	8.67	75.17
0.25	8.55	73.10
0.50	7.99	63.84
0.75	7.50	56.25
1.00	7.21	51.98

5.4 Conclusions

- SANS provides quantitative information about the structural changes of mixed micelles of 12-4-12 MEA and C₁₂DMEAB.
- Micelles of only C₁₂DMEAB are nearly spherical and shape becomes increasingly more ellipsoidal with increase in mole fraction of 12-4-12 MEA in mixed surfactant system.
- The average degree of micelle ionization decreases with increasing mole fraction of 12-4-12 MEA in mixed micellar system.
- The Kraft temperature of mixed surfactant system was observed to increase when mole fraction of 12-4-12 MEA increased.
- Foamability was observed to decrease and foam stability was observed to increase with increase in mole fraction of 12-4-12 MEA indicating increase in the stability of micelles.
- Oil solubilization capacity was also observed to increase with increased fraction of 12-4-12 MEA in mixed surfactant system.

5.5 Literature Cited

1. Holland P. M., Rubingh D. N., *Mixed Surfactant Systems*, Am. Chem. Soc., Washington, DC, **1992**.
2. Stubbs G.W., Gilbert S. H., Litman B.J., *BioChim. BioPhys. Acta.*, **1976**, 45, 425.
3. Christian S. D., Scamehron J. F., *Solubilization in surfactant Aggregates*, Marcel Dekker, New York, Vol.55, **1995**.
4. Ogino K., Abe M., *Mixed Surfactant Systems*, Marcel Dekker, New York, **1993**.
5. Karaborni S., Esselink K., Jhilbers P. A., Smit B., Karthaus J., Van Os N. M., Zana R., *Science*, **1994**, 266, 254.
6. Sharma V., Borse M., Dave K., Pohnerkar J., Prajapati A., Devi S., *J. Dispersion Sci. Technol.*, **2005**, 26, 421.
7. Bunton A., Schaak L., Stam M. F., *J. Org. Chem.*, **1971**, 36, 2364.
8. Menger F. M., Littau C. A., *J. Am. Chem. Soc.*, **1993**, 115, 10083.
9. Menger F. M., Littau C. A., *J. Am. Chem. Soc.*, **1991**, 113, 145.
10. Rosen M. J., *Chemtech*, **1993**, 23, 3033.
11. Zana R., *Adv. in Colloid and Interface Sci.*, **2002**, 97, 203.
12. Alami E., Levy H., Zana R., Skoulios A., *Langmuir*, **1993**, 9, 940.
13. Rosen M. J., Mathias J. H., Davenport L., *Langmuir*, **1999**, 15, 7340.
14. Wettig S. D., Verrall R. E., *J. Colloid Interface Sci.*, **2001**, 235, 310.
15. Wettig S. D., Nowak P., Verrall R. E., *Langmuir*, **2002**, 18, 5354.
16. Zana R., Talmon Y., *Nature*, **1993**, 362, 228.
17. Zana R., Esumi K., Uneno M. (Eds.) *Structure Performance Relationship in Surfactants*, Marcel Dekker, New York, **1997**.
18. Zhao J., Christian S. D., Fung B. M., *J. Phys. Chem. B*, **1998**, 102, 7613.
19. Schosseler F., Anthony O., Beinert G., Zana R., *Langmuir*, **1995**, 11, 3347.
20. De S., Aswal V. K., Goyal P. S., Bhattacharya S., *J. Phys. Chem. B*, **1997**, 101, 5639.

21. Lusvardi K. M., Full A. P., Kaler E. W., *Langmuir*, **1995**, 11, 487.
22. Junquera E., Ortega F., Aicart E., *Langmuir*, **2003**, 19, 4923.
23. Borse M., Sharma V., Aswal V. K., Pokhariyal N. K., Joshi J. V., Goyal P. S., Devi S., *Phys. Chem. Chem. Phys.*, **2004**, 6, 3508.
24. Borse M., Sharma V., Aswal V. K., Goyal P. S., Devi S., *J. Colloid and Interface Sci*, **2005**, 284, 282.
25. Borse M., Devi S., *Colloid and Surface A.*, **2004**, 245, 1.
26. Sharma V., Borse M., Aswal V. K., Pokhariyal N. K., Joshi J. V., Goyal P. S., Devi S., *J. Colloid and Interface Sci.*, **2004**, 277, 450.
27. Shah D. O., *J. Colloid and Interface Sci*, **1971**, 37, 744.
28. Patist A., Devi S., Shah D. O., *Langmuir*, **1999**, 15, 7403.
29. Aswal V. K., Goyal P. S., *Current Science*, **2000**, 79, 947.
30. Shinoda K., Halo M., Hayashi T., *J. Phys. Chem.*, **1972**, 76, 909.
31. Clint J. H., *J. Chem. Soc., Faraday Trans*, **1975**, 1, 1327.
32. Goyal P. S., Dasannacharya B. A., Kelkar V. K., Manohar C., Rao K. S., Valaulikar B. S., *Physica B*, **1991**, 174, 196.
33. Hayter J. B., Penfold J., *J. Mol. Phys.*, **1981**, 2, 109.